Pakistan J. Zool., vol. 54(4), pp 1849-1857, 2022 DOI: https://dx.doi.org/10.17582/journal.pjz/20200618170629

L237P Substitution in the *UROS* Gene Causes X-linked Recessive Congenital Erythropoietic Porphyria in Pakistani Consanguineous Family Through Altered Uroporphyrinogen III Binding

Roshana Mukhtar[1], Shaheen Shahzad[1]*, Sajid Rashid[2], Maryam Rozi[2], Madiha Rasheed[3], Imran Afzal[4] and Pakeeza Arzoo Shaiq[5]

[1]*Genomics Research Lab, Department of Biological Sciences, International Islamic University, Islamabad*
[2]*National Centre of Bioinformatics, Quaid-i-Azam University, Islamabad*
[3]*Beijing Key Laboratory for Separation and Analysis in Biomedicine and Pharmaceuticals, School of Life Sciences, Beijing Institute of Technology, Beijing, China.*
[4]*Department of Biology, Lahore Garrison University, Lahore*
[5]*University Institute of Biotechnology and Biochemistry, Pir Mehr Ali Shah Arid Agriculture University, Rawalpindi*

Article Information
Received 18 June 2020
Revised 30 July 2020
Accepted 10 November 2020
Available online 24 August 2021 (early access)
Published 22 April 2022

Authors' Contribution
RM identified the family and collected samples. SS supervised the study. PAS, SS and RM did experiments and interpret the results. SR did bioinformatic analysiis of the data and its interpretation. M Rozi compiled the bioinformatic data. M Rasheed and M Rozi prepared the figures. IA and SS wrote, edited and proofread the manuscript.

Key words
Congenital erythropoietic porphyria, Mutation, UROS, Recessive, Substitution

ABSTRACT

Congenital erythropoietic porphyria (CEP) is an inherited heterogeneous metabolic disorder caused by an abnormal activity of uroporphyrinogen-III synthase (UROS), aminolevulinic acid and *GATA1* (GATA binding factor 1) genes. The fundamental genetic cause of CEP has been linked to a sequence variant of *UROS* on chromosome 10q252-q263. The enzyme catalyzes the fourth step of heme synthesis pathway. The present study focused on the clinical assessment of CEP affected individuals in a Pakistani consanguineous family by Sanger sequencing of *UROS* gene to identify potential pathogenic sequence variants. CEP patients were identified using successive clinical tests. Blood samples of patients were collected and processed for genomic DNA extraction followed by Sanger sequencing to identify pathogenic mutations in UROS gene. Sequence analysis revealed a pathogenic missense mutation (c.935T>C [p. L237P]) in the exon 10.The sequence was further analysed *in-silico* to determine the effect of pathogenic mutation on protein structure. *In-silico* analysis and comparison between $UROS^{L237P}$ and $UROS^{WT}$ 3-dimensional structures revealed remarkable changes in the binding site of Urogen (3-[7, 12, 18-tris (2-carboxyethyl)-3, 8, 13, 17-tetrakis (carboxymethyl) 5, 10, 15, 20, 21, 22, 23, 24-octahydroporphyrin-2-yl] propanoic acid) due to narrowing of domain-I and domain-II (18.46-12.17Å) of $UROS^{L237P}$ as compared to $UROS^{WT}$. This suggests that UROS L237P mutation may influence heme biosynthesis mechanism through altered Urogen binding mechanism. Therefore, we propose that the newly identified pathogenic missense variant (c.935T>C [p.L237P]) p.Gly439Ser) of the *UROS* gene causes CEP in a large consanguineous Pakistani family, possibly by hindering heme biosynthesis mechanism through altered Urogen binding mechanism.

INTRODUCTION

Congenital erythropoetic porphyria (CEP) is an inherited metabolic disorder that occurs due to malfunctioning of UROS enzyme causing excessive accumulation and excretion of porphyrins and their toxic precursors (Szlendak *et al*., 2016). It is a rare genetic disorder inherited either as autosomal recessive or X-linked trait due to mutations in *UROS* and *GATA* 1 genes (Di Pierro *et al*., 2016. The main symptoms of CEP include harsh cutaneous photo-sensitivity with damage and sub-epidermal blistering (Poh-Fitzpatrick, 1998), scarring, erythrodontia (Darwich *et al*., 2011), mild bone loss and expansion of the bone marrow (Berry *et al*., 2005), eye sight problem (Agarwal *et al*., 2015), pink to dark red staining of the urine.

* Corresponding author: drshaheen@iiu.edu.pk
0030-9923/2022/0004-1849 $ 9.00/0

Abbreviations
CEP, congenital erythropoetic porphyria; ALAS, aminolevulinic acid synthase; HMB, hydroxy methyl bilane; HGMD, human gene mutation database; PCR, polymerase chain reaction; SIFT, sorting intolerant from tolerant; PolyPhen-2, polymorphism phenotyping v2; PDB, protein data bank.

(Szlendak *et al*., 2016), thrombocytopenia (Ged *et al*., 2004), and disturbance in accumulated porphyrin, leading to the development of cutaneous reactions (Thunell, 2000). Besides this, there is rapid development of cutaneous vesicles with increased skin fragility and bullae on the face and hands (Baran *et al*., 2013) with variable hematological symptoms, which includes asymptomatic microcytic anemia, hemolytic anemia and pancytopenia (Egan *et al*., 2015).The disease may be hepatic, erythropoeitic, organ system, cutaneous and neuropsychiatric, depending upon the biochemical problems at different stages of heme biosynthesis pathway (Scarlett and Brenner, 1998).

There are various enzymes that catalyze different steps of heme synthesis. Aminolevulinic acid synthase (ALAS) is the enzyme which catalyzes the first rate limiting step, whereas UROS enzyme in cytosol is involved in the fourth step of heme pathway (Ponka, 1997). UROS enzyme helps in the formation of uroporphyrinogen III by rearranging and cyclising the linear HMB (hydroxy methyl bilane). URO I and COPRO I are toxic isomers, which are abnormally produced due to defect in the enzyme (Di Pierro *et al*., 2016).

CEP is a genetically heterogenic state that occurs due to mutations in different genes. Acquired *GATA1* and *UROS* gene mutations have been reported in the CEP patients (Sarkany *et al*., 2011). About 95% cases of CEP occur due to genetic mutation in the *UROS* gene and are responsible for the disease manifestations (Di Pierro *et al*., 2016). *UROS III* was identified in 1998, being approximately 34 kb long and having 10 exons, out of which 1 and 2A are untranslated (non-coding) exons. The remaining 9 exons (2B to 10) are translated into a protein (Aizencang *et al*., 2000). *UROS* gene encodes a protein of 265 amino acids and is chromosomally located at the position "10q252–q263" (Astrin *et al*., 1991). It is a monomeric enzyme with a molecular weight of 29 kDa, purified and characterized from human erythrocyte (Tsai *et al*., 1987). The protein structure shows two domains and each domain contains a parallel beta-sheet surrounded by alpha-helices, linked with each other by a two-strand antiparallel beta-ladder (Mathews *et al*., 2001). Nuclear Magnetic Resonance (NMR) has revealed the interaction of the enzyme with a ligand through chemical shift perturbation. The active location was mapped in the cleft section between structural domains 1 and 2 where conserved residues were clustered (Cunha *et al*., 2008). Approximately 49 mutations have been reported in *UROS* gene responsible for CEP, based on literature and "Human Gene Mutation Database (HGMD)", (http://www.hgmd.cf.ac.uk/ac/index.php). Most of these mutations are dispersed all over the coding regions of the *UROS* gene and some are in the promoter region (Solis *et al*., 2001).

Point mutations have been reported mostly in *UROS* gene. Deletions and insertions cause the rearrangements in genes and only 6 mutations of this category have been reported, with 56% of UROS mutations being missense. Other reported mutation types include one non-sense mutation, five mutations linked to splicing defects, six in regulatory region of the gene, four belonging to the group of deletions, four to insertions groups , and two from in-dels group (ben Bdira *et al*., 2014).

This study focused on the clinical assessment of individuals affected with CEP in a Pakistani consanguineous family to determine the possible involvement of *UROS* gene mutation in the CEP manifestation. The *UROS* gene sequence was obtained and analyzed *in silico* to compare the mutant $UROS^{L237P}$ structural abnormalities to the wild type $UROS^{WT}$ gene structure in order to identify the possible role of the mutation in CEP manifestation.

MATERIALS AND METHODS

Family recruitment and ethical approval

The study was approved by Ethical Review Committee of the International Islamic University, Islamabad, Pakistan. A written informed consent was provided by all the participants and legal guardians. The consanguineous family presently studied is from Punjab province of Pakistan (Fig. 1). The family pedigree of this large family indicated an X-linked recessive CEP. Affected individuals were examined by a physician for the disease phenotype and detailed clinical history was established (unpublished data). The clinical symptoms are summarized below.

1. Skin abnormalities (harsh cutaneous photosensitivity with blistering, scarring)
2. Erythrodontia (reddish discoloration of the teeth)
3. Defect in the heme synthesis within the red blood cells of bone marrow (which leads to anemia and reddish colour urine
4. Hypertrichosis (excessive hair growth on face and hands)
5. Liver and spleen problems
6. Hands mutilating deformities of fingers with no finger prints

After clinical examination, the phenotype of patients clearly indicated CEP with typical cutaneous lesions and hypertrichosis.

Clinical tests

Clinical tests were performed to confirm the type of porphyria. Wood's lamp test was performed to confirm the CEP as the test involves the UV light and it is a diagnostic marker test for the CEP (Bhavasar *et al*., 2011).

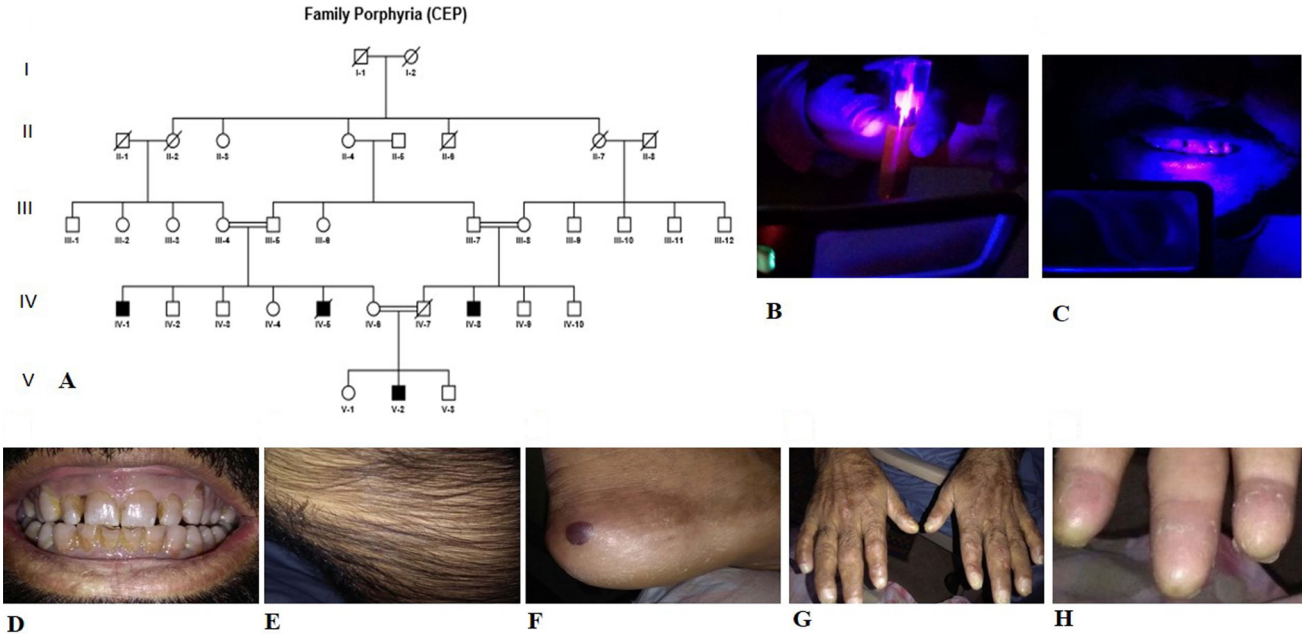

Fig. 1. (A) Pedigree of the 5-generation consanguineous Pakistani family, showing features of X-linked recessive Congenital Erythropoietic Porphyria. Consanguineous unions are shown through double lines. Males and females are represented using squares and circles respectively. The affected and unaffected family members are shown using filled and clear symbols respectively, while a deceased individual is represented through a diagonal line. (B) Urine under wood lamp test. (C) Teeth colour under wood lamp test. (D-H) the clinical appearance of the affected persons (D) Eryhtrodondia, (E) Hypertrichosis, (F) Blisters formation on skin exposed to sunlight, (G) Blister healing with scarring, (H) Hands mutilating deformities of fingers with no finger prints.

DNA extraction and amplification

Genomic DNA was extracted from peripheral leucocytes of the affected (IV-I, IV-8, V-2) and unaffected (III-4, IV-4, IV-6, VI) family members using organic DNA extraction protocol (Wood, 1983). DNA quantification was performed using Nanodrop (AUVS. 102/avans). DNA concentration was adjusted to 40-50 ng/L for its amplification. For PCR amplification, primers were designed for *UROS* gene containing 10 exons by using primer3 software and gene was amplified using Thermal Cycler (BioRad-T100) using standard PCR conditions (Rozen and Skaletsky, 2000).

The *UROS* gene on chromosome 10q252–q263 (NM_001324036) was sequenced for all the available affected and normal persons of the family. DNA purification was performed with a commercially kit (Axygen Inc., CA, USA) and sequencing was also done commercially using the BigDye Terminator v3.1 Cycle Sequencing Kit, together with an ABI Prism 310 Genetic Analyzer (Applera, Foster City, CA, USA). Mutation was identified using BioEdit sequence alignment editor version 6.0.7.

Bioinformatics analysis

SIFT and polyphen scoring

Sorting Intolerant from Tolerant (SIFT) and(Polymorphism Phenotyping v2 (PolyPhen-2), were used to characterize missense variation and examine the possible effect of amino acid substitutions on the stability and function of proteins.

Data set

The crystal structure of human UROS^{WT} (PDB ID: 1JR2) was retrieved using protein data bank (PDB) (Berman *et al*., 2000). The energy minimization procedure was performed through UCSF Chimera 1.5.6 (Pettersen *et al*., 2004) by means of conjugate gradient method and Amber force field. 3-dimensional structure of UROS^{L237P} was predicted by Modeller 9.14 (Šali *et al*., 1995) using 1JR2 structure as template. The predicted 3-dimensional structure was confirmed by MolProbity (Darwich *et al*., 2011) analysis, followed by structure optimization through WinCoot (Emsley *et al*., 2010). 2D structure of UROGEN (PubChem ID: 1179) was retrieved through PubChem database (Hanwell *et al*., 2012) and converted into PDB format through UCSF Chimera. Avogadro tool was utilized to obtain proper protonation

and stereo-isomerization state of UROGEN using GAFF force field (Kim *et al*., 2015).

Molecular docking analysis

PatchDock was used to perform molecular docking analysis of $UROS^{WT}$ and $UROS^{L237P}$ structures against UROGEN (Schneidman-Duhovny *et al*., 2005) and FireDock (Andrusier *et al*., 2007) servers. PatchDock docking was done in three stages: First, the detection of geometric patches through segmentation method was done; second, surface matching and filtering was performed; and in the final stage, scoring was done. In the process of docking, hundreds of binding poses are produced and best docked structure is considered with minimum energy pose (Huang and Zou, 2010). Through UCSF Chimera ver 1.5.6 and LigPlus the comprehensive interactions were characterized (Laskowski and Swindells, 2011).

RESULTS

Clinical profile

The result of Wood's lamp test revealed that the urine sample of the affected members of the family under UV light had red color due to the presence of excess porphyrin compounds. The teeth color appeared pink to red due to the accumulation of porphyrin compounds in teeth tissues during teeth development (Fig. 1).

The characteristic symptoms in the affected members of the family included: Skin abnormalities (harsh cutaneous photo-sensitivity with blistering, scarring), Erythrodontia (reddish discoloration of the teeth), heme synthesis defect within the red blood cells of bone marrow (leading to anemia and reddish colour urine), Hypertrichosis (hair growth increases on face and hands), and hands mutilating deformities of fingers with no finger prints. The symptoms were present in all affected individuals by birth, but the severity of symptoms was variable among affected patients and become more severe due to sun exposure, which is supposed to be because of reduced enzymatic activity of UROS. One of the members, the oldest among the affected ones, h also had liver and spleen problem.

Mutation screening

Sanger sequencing of the *UROS* gene carried out using DNA samples from all available family members (Fig. 1), revealed a reported missense mutation c.935T>C (p. Leu237Pro). The mutation segregated in the family with the disease phenotype (Fig. 2a-2c). Affected individuals were homozygous for the altered allele (CC), the parents were heterozygous carriers (CT), and the unaffected children were either heterozygous (CT) or homozygous for the wild-type allele (TT) (Fig. 2a-2c). The disease-causing mutation (c.935T>C) resides in exon 10 of the *UROS* gene (NM_001324036) which causes Leucine to Proline substitution at position 237 (p. Leu237Pro) within the amino acid sequence of the translated UROS protein. This mutation occurs in the coding region, predicted to be damaging according to PolyPhen2 (http: //genetics.bwh.harvard.edu/pph), SIFT/PROVEAN (http://sift.jcvi.org). After mutation screening, SIFT and Polyphen test was performed to check the type of mutation and also predict the effect of mutation on the structure and function of the protein. The mutation is highly deleterious and has effect on protein structure and function as the scores lies in the damaging region and predicted to have negative effect on the protein function, as predicted through SIFT and Polyphen scores (Tables I and II).

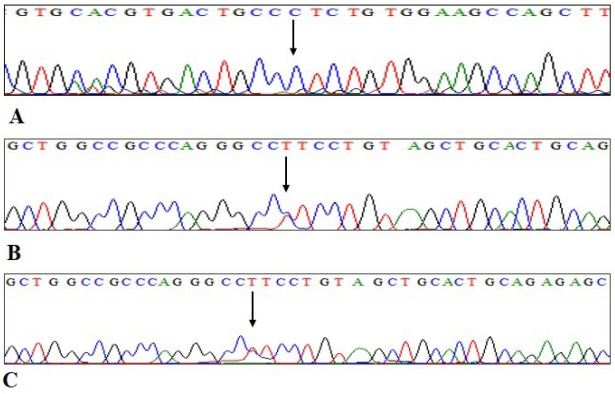

Fig. 2. Sequence analysis of the *UROS* gene revealing the mutation c.935T>C (p.Leu237Pro). (A) shows the nucleotide sequence of an affected individual, (B) a heterozygous carrier, (C) a homozygous normal individual. The arrow represents the missense mutation.

Table I. SIFT analysis.

ENSP	Position	Reference	Substitution	Prediction	SIFT score	Median information content
ENSP 00000357787	237	L	P	damaging	0.01	1.51

Table II. Polyphen analysis.

Mutation	Hum div score	Hum var score
L237P	0.999 Damaging	0.995 Damaging

Bioinformatics analysis

3-dimensional structure superimposition for $UROS^{WT}$ and $UROS^{L237P}$ structures showed similar folds adapted by both structures through sharing a well-conserved helix-loop-helix structure, oriented by the association

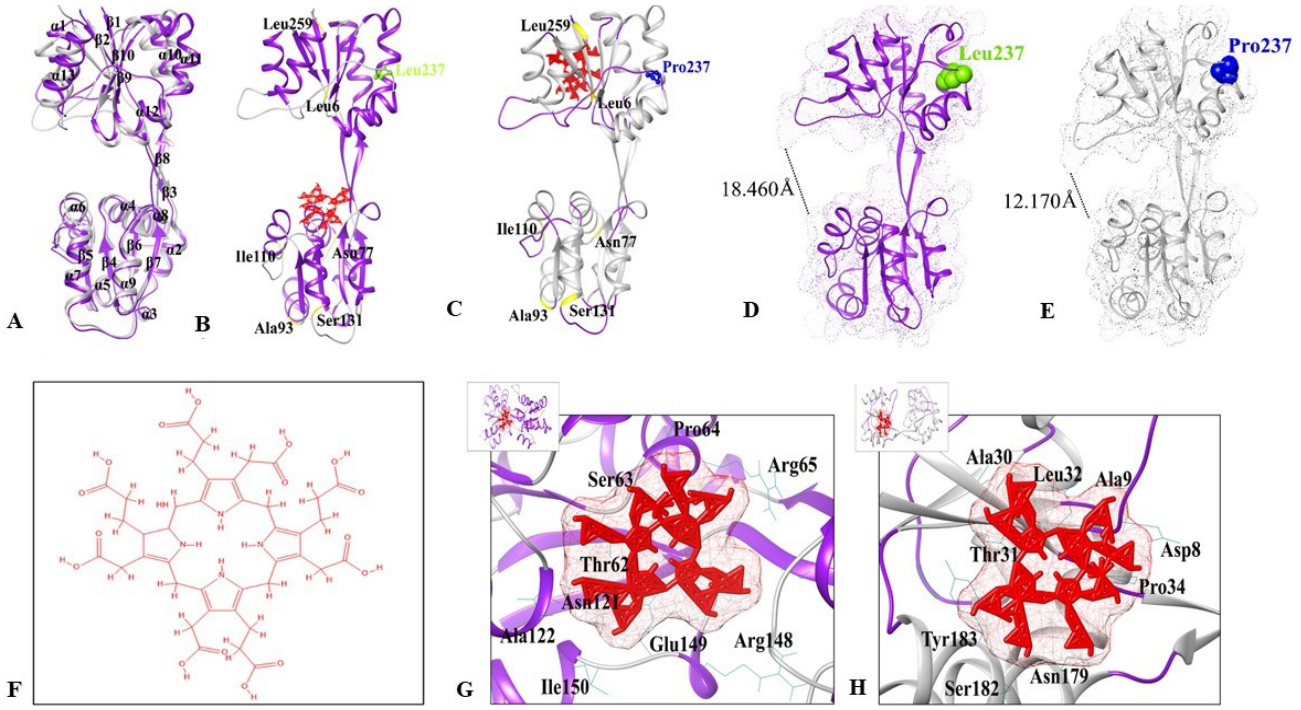

Fig. 3. Structure analysis of UROS^{WT} and UROS^{L237P}. (A) Superimposition of UROS^{WT} and UROS^{L237P} structures. UROS^{WT} is indicated in purple color, while UROS^{L237P} is indicated in grey color. (B) Topview representation of UROS^{WT}-Urogen complex in purple color. (C) UROS^{L237P} -Urogen complex in grey color. Urogen is shown in red colored stick representation. Leu237 and Pro237 residues are indicated by green and blue spheres. (D-E) Structural comparison. (D) UROS^{WT} is indicated in purple color, (E) UROS^{L237P} model is indicated in grey color. Leu237 and Pro237 residues are indicated by green and blue spheres. Dotted lines indicate distance between adjacent residues. Bond length is indicated in Å. (F) Binding mode analysis of UROS^{WT} and UROS^{L237P}. (G) 2D structure of Urogen (3-[7, 12, 18-tris (2-carboxyethyl)-3, 8, 13, 17 tetrakis (carboxymeth-yl)-5, 10, 15, 20, 21, 22, 23, 24 octahydroporphyrin-2-yl] propanoicacid). (H) UROS^{WT} (purple) binding with Urogen (red). (C) UROS^{L237P} (grey) binding with Urogen (red). The interacting residues are labelled in black color with wire representation.

of α-helices at the outer periphery; while the inner core mainly consisted of β-sheets (Fig. 3a). Overall, UROS^{WT} and UROS^{L237P} revealed 12 α-helices and 10 β-strands. Due to a high structural homology between UROS^{WT} and UROS^{L237P} models, the inner cores were measured between two globular regions.

An RMSD value of 0.968Å indicated significant change in the helical conformation at structural level. The change in helical conformation of UROS^{L237P} involving residues LEU6, ASN77, ALA93, ILE110, SER137 and LEU259 led to the elongation of loop region in UROS^{WT} (Fig. 3b and 3c). In comparison to UROS^{WT}-Urogen, the prominent structural differences were observed at the Urogen binding site of UROS^{L237P}-Urogen. The structure comparison exhibited notable changes in the bond length of UROS^{L237P} as compared with UROS^{WT}. In UROS^{WT}, the bond length between C13 and C110 was 18.46Å, whereas in UROS^{L237P}; bond length was reduced to 12.17Å (Fig. 3d and 3f).

UROS^{WT} and UROS^{L237P}structures in complex with Urogen were assessed based on the values of their binding energy. PatchDock specific energy value for UROS^{WT} and Urogen complex was -74.56 kcal/mol, while for UROS^{L237P}–Urogen complex, binding energy value was -70.86 kcal/mol. In case of UROS^{WT}–Urogen complex, THR62, SER63, PRO64, ARG65, GLY100, GLY120, ASN121, ALA122, ARG148, GLU149, ILE150, TYR168, THR170 and VAL99 residues were involved in hydrophobic bonding with Urogen (Fig. 3g and 3h). In UROS^{L237P}-Urogen complex, ASP8, ALA9, ILE20, ALA30, THR31, LEU32, PRO34, ASN179, SER182, TYR183, GLN186 and GLN187 residues of UROS^{L237P} were involved in hydrophobic interactions with Urogen (Fig. 3g-3h).

DISCUSSION

The present study was conducted to identify the *UROS* gene mutation as a causative agent in the inherited CEP and to predict the mutated structure of

the gene with docking analysis. Here, we describe a large consanguineous Pakistani kindred affected with rare CEP caused by a known but pathogenic missense mutation (c.935T>C [p.Leu237Pro]) in the *UROS* gene that encodes uroporphyrinogen III synthase. This was previously reported as a missense variant (Moghbeli *et al*., 2012). Presently we report the pathogenic disease-causing mutation of the *UROS* gene for the first time in the Pakistani family and its association with X-linked recessive CEP. All the affected persons were homozygous for the missense mutation in L237P and their consanguineous parents were shown to be heterozygous for the same mutation.

In CEP, a broad variation has been described regarding the extent and severity of clinical manifestation. The symptoms reported in earlier studies were cutaneous photo-sensitivity, porphyrin overload leading to metabolic disturbance; Erythrodontia and dentine disorders, sub-epidermal blistering; hyperorthokeratosis; sclerosis in the skin layer dermis; disappearance of sweat glands; more fragile and blisters on skin of hands and face upon sun exposure; hypo and hyper-pigmentation on skin, abnormal growth of hairs on hands, face and extremities, etc.; scarring alopecia; significant mutilations; contraction and shortening of the digits and limb and facial disfigurement, i.e., loss of facial features; vitamin D deficiency; shortening of stature and backbone problems; abnormal enlargement of spleen; disturbed liver function; and common mild to severe anemia among the patients (Poh-Fitzpatrick, 1986; Freesemann *et al*., 1997; Berry *et al*., 2005; Arunachalam *et al*., 2013; Baran *et al*., 2013; Verma *et al*., 2014; Szlendak *et al*., 2016). One unique feature that affected individuals of the studied family had no finger prints which may be due to ectopic eczema. The finger prints were not missing by birth. As the affected person grows up and the severity of the disease increases due to regular exposure to sun light, more blistering, scarring and sclerosis problems starts appearing on their finger's tips.

Several studies have reported molecular heterogeneity in CEP in which *UROS* gene mutations were identified, including missense, nonsense, frameshift and splice-site mutations (Deybach *et al*., 1990; Boulechfar *et al*., 1992; Warner *et al*., 1992; Tanigawa *et al*., 1995; Xu *et al*., 1995; Tezcan *et al*., 1998; Solis *et al*., 2001; Shady *et al*., 2002).

The leucin residue at the 237 position is conserved in mouse, rat, zebra fish, and some bacteria. Other amino acids encountered at this position are isoleucin (e.g. in *Xenopus laevis* or *Gallus gallus*), glutamine (*Drosophila melanogaster*) and threonine (*Schizosaccharomyces pombe*), which are all large and uncharged amino acids. By contrast, the mutation replacing leucine residue with proline (L237P) resulted in secondary amino acid (Yisgedu *et al*., 2010). The resulting circular structure greatly reduced the structural flexibility and, thus, a leucin to proline substitution at this site may result in an important structural alteration with subsequent disturbance of the encoded protein (Wiederholt *et al*., 2006). The protein structure of the *UROS* comprises of two domains that exhibit similarity at sequence level. To check the effect of mutation on protein structure and function, SIFT and Polyphene tools were used, which revealed damaging effect of mutation. UROS protein structural studies demonstrated that Leucine residue at 237 position might have a role as a hydrogen bond donor and acceptor in the UROS protein active site (Mathews *et al*., 2001). The structural changes at the active site might result in the modulation of enzyme activity (Schubert *et al*., 2008). Interestingly, in $UROS^{L237P}$, Urogen (uroporphyrinogen III) binding was completely shifted as compared to $UROS^{WT}$. In $UROS^{WT}$-Urogen complex, active site THR62, SER63, PRO64, ARG65, GLY100, GLY120, ASN121, ALA122, ARG148, GLU149, ILE150, TYR168, THR170 and VAL99 residues lying at the cleft between domain-I and II (Mathews *et al*., 2001) were involved in Urogen binding. In contrast, $UROS^{L237P}$-Urogen complex exhibited the involvement of ASP8, ALA9, ILE20, ALA30, THR31, LEU32, PRO34, ASN179, SER182, TYR183, GLN186 and GLN187 residues of $UROS^{L237P}$ in the interaction. Predicted Urogen binding site for human $UROS^{WT}$ is highly similar to the experimentally mapped site of Urogen and *T. thermophilus* UROS (Schubert *et al*., 2008). These data clearly demonstrate that L237P point mutation in *UROS* may influence heme biosynthesis mechanism through altered Urogen binding.

CONCLUSION

We have identified a pathogenic missense variant (c.935T>C [p.L237P]) p.Gly439Ser) of the *UROS* gene as a causative agent for CEP in a large consanguineous Pakistani kindred. L237P induced a binding shift of Uroporphyrinogen III due to narrowing of domain-I and domain-II (18.46-12.17Å) of $UROS^{L237P}$ as compared to $UROS^{WT}$. For disease management, mutation analysis of various genes causing CEP is important. Although, presently no specific therapy is available for the treatment of CEP, different options for the treatment of CEP are in progress. Taken together, our findings are expected to strengthen the role of *UROS* mutation as a cause of CEP, and provide further facts for the lack of genotype-phenotype correlation and clinical variability in patients with *UROS* mutation and CEP.

ACKNOWLEDGEMENTS

The Authors acknowledge Dr. Nigar Kunwal, Associate Physician Dermatologist facilitated in clinical diagnosis of the disease. Muhammad Mobeen Zafar and Ms. Samra Batool, Research Scholars provided guidance during lab experiments.

Statement of all funding sources for this work

None

Statement of conflict of interest

The authors have no conflict of interest to declare.

REFERENCES

Agarwal, S., Majumder, P.D., Srinivasan, B. and Iyer, G., 2015. Scleral necrosis in congenital erythropoietic porphyria: A case report and review of the literature. *Oman J. Ophthalmol.,* **8**: 200. https://doi.org/10.4103/0974-620X.169904

Aizencang, G., Solis, C., Bishop, D.F., Warner, C. and Desnick, R.J., 2000. Human uroporphyrinogen-III synthase: genomic organization, alternative promoters, and erythroid-specific expression. *Genomics*, **70**: 223-231. https://doi.org/10.1006/geno.2000.6373

Andrusier, N., Nussinov, R. and Wolfson, H.J., 2007. FireDock: fast interaction refinement in molecular docking. *Proteins,* **69**: 139-159. https://doi.org/10.1002/prot.21495

Arunachalam, M., Bassi, A., Galeone, M., Scarfi, F. and Difonzo, E., 2013. Scleroderma-like hands in a 16 year old boy. *JAMA Dermatol.,* **149**: 969-970. https://doi.org/10.1001/jamadermatol.2013.3370a

Astrin, K.H., Warner, C.A., Yoo, H.-W., Goodfellow, P.J., Tsai, S.-F. and Desnick, R.J., 1991. Regional assignment of the human uroporphyrinogen III synthase (UROS) gene to chromosome 10q25. 2→ q26. 3. *Hum. Genet*., **87**: 18-22. https://doi.org/10.1007/BF01213085

Baran, M., Eliaçık, K., Kurt, İ., Kanık, A., Zengin, N. and Bakiler, A.R., 2013. Bullous skin lesions in a jaundiced infant after phototherapy: a case of congenital erythropoietic porphyria. *Turk. J. Pediatr.,* **55**: 218. https://doi.org/10.1093/hmg/ddu298

ben Bdira, F., González, E., Pluta, P., Laín, A., Sanz-Parra, A., Falcon-Perez, J.M. and Millet, O., 2014. Tuning intracellular homeostasis of human uroporphyrinogen III synthase by enzyme engineering at a single hotspot of congenital erythropoietic porphyria. *Hum. mol. Genet.,* **23**: 5805-5813.

Berman, H.M., Westbrook, J., Feng, Z., Gilliland, G., Bhat, T.N., Weissig, H., Shindyalov, I.N. and Bourne, P.E., 2000. The protein data bank. *Nucl. Acids Res.,* **28**: 235-242.

Berry, A.A., Desnick, R.J., Astrin, K.H., Shabbeer, J., Lucky, A.W. and Lim, H.W., 2005. Two brothers with mild congenital erythropoietic porphyria due to a novel genotype. *Arch Dermatol.,* **141**: 1575-1579. https://doi.org/10.1001/archderm.141.12.1575

Bhavasar, R., Santoshkumar, G. and Prakash, B.R., 2011. Erythrodontia in congenital erythropoietic porphyria. *J. Oral Maxillofac. Pathol*., **15**: 69. https://doi.org/10.4103/0973-029X.80022

Boulechfar, S., Da Silva, V., Deybach, J.-C., Nordmann, Y., Grandchamp, B. and de Verneuil, H., 1992. Heterogeneity of mutations in the uroporphyrinogen III synthase gene in congenital erythropoietic porphyria. *Hum. Genet.,* **88**: 320-324. https://doi.org/10.1007/BF00197267

Cunha, L., Kuti, M., Bishop, D.F., Mezei, M., Zeng, L., Zhou, M.M. and Desnick, R.J., 2008. Human uroporphyrinogen III synthase: NMR-based mapping of the active site. *Proteins,* **71**: 855-873. https://doi.org/10.1002/prot.21755

Darwich, E., Guilabert, A., Aceituno, A., Mas, N., To-Figueras, J. and Herrero, C., 2011. Congenital erythropoietic porphyria and Parkinson's disease: clinical association in a patient with a long-term follow-up. *Eur. J. Dermatol*., **21**: 613-614. https://doi.org/10.1684/ejd.2011.1329

Deybach, J., De Verneuil, H., Boulechfar, S., Grandchamp, B. and Nordmann, Y., 1990. Point mutations in the uroporphyrinogen III synthase gene in. *Blood*, **75**: 1763-1765. https://doi.org/10.1182/blood.V75.9.1763.bloodjournal7591763

Di Pierro, E., Brancaleoni, V. and Granata, F., 2016. Advances in understanding the pathogenesis of congenital erythropoietic porphyria. *Br. J. Haematol.,* **173**: 365-379. https://doi.org/10.1111/bjh.13978

Egan, D.N., Yang, Z., Phillips, J. and Abkowitz, J.L., 2015. Inducing iron deficiency improves erythropoiesis and photosensitivity in congenital erythropoietic porphyria. *Blood,* **126**: 257-261. https://doi.org/10.1182/blood-2014-07-584664

Emsley, P., Lohkamp, B. and Scott, W.G., Cowtan, K., 2010. Features and development of Coot. *Acta Crystallogr. D: Biol. Crystallogr.,* **66**: 486-501. https://doi.org/10.1107/S0907444910007493

Freesemann, A., Bhutani, L., Jacob, K. and Doss,

M., 1997. Interdependence between degree of porphyrin excess and disease severity in congenital erythropoietic porphyria (Günther's disease). *Arch Dermatol. Res.,* **289**: 272-276. https://doi.org/10.1007/s004030050192

Ged, C., Mégarbané, H., Chouery, E., Lalanne, M., Megarbane, A. and de Verneuil, H., 2004. Congenital erythropoietic porphyria: Report of a novel mutation with absence of clinical manifestations in a homozygous mutant sibling. *J. Invest. Dermatol.,* **123**: 589-591. https://doi.org/10.1111/j.0022-202X.2004.23401.x

Hanwell, M.D., Curtis, D.E., Lonie, D.C., Vandermeersch, T., Zurek, E. and Hutchison, G.R., 2012. Avogadro: An advanced semantic chemical editor, visualization, and analysis platform. *J. Cheminform.,* **4**: 17. https://doi.org/10.1186/1758-2946-4-17

Huang, S.-Y. and Zou, X., 2010. Advances and challenges in protein-ligand docking. *Int. J. Mol. Sci.,* **11**: 3016-3034. https://doi.org/10.3390/ijms11083016

Kim, S., Thiessen, P.A., Bolton, E.E., Chen, J., Fu, G., Gindulyte, A., Han, L., He, J., He, S. and Shoemaker, B.A., 2015. PubChem substance and compound databases. *Nucl. Acids Res.,* **44**: D1202-D1213. https://doi.org/10.1093/nar/gkv951

Laskowski, R.A. and Swindells, M.B., 2011. LigPlot+: multiple ligand–protein interaction diagrams for drug discovery. *J. Chem. Inf. Model*, **51**: 2778-2786. https://doi.org/10.1021/ci200227u

Mathews, M.A., Schubert, H.L., Whitby, F.G., Alexander, K.J., Schadick, K., Bergonia, H.A., Phillips, J.D. and Hill, C.P., 2001. Crystal structure of human uroporphyrinogen III synthase. *EMBO J.,* **20**: 5832-5839. https://doi.org/10.1093/emboj/20.21.5832

Moghbeli, M., Maleknejad, M., Arabi, A., Abbaszadegan, M.R., 2012. Mutational analysis of uroporphyrinogen III cosynthase gene in Iranian families with congenital erythropoietic porphyria. *Mol. Biol. Rep.,* **39**: 6731-6735. https://doi.org/10.1007/s11033-012-1497-z

Pettersen, E.F., Goddard, T.D., Huang, C.C., Couch, G.S., Greenblatt, D.M., Meng, E.C. and Ferrin, T.E., 2004. UCSF Chimera a visualization system for exploratory research and analysis. *J. Comput. Chem.,* **25**: 1605-1612. https://doi.org/10.1002/jcc.20084

Poh-Fitzpatrick, M.B., 1986. The erythropoietic porphyrias. *Dermatol. Clin.,* **4**: 291-296. https://doi.org/10.1016/S0733-8635(18)30833-7

Poh-Fitzpatrick, M.B., 1998. Clinical features of the porphyrias. *Clin. Dermatol.,* **16**: 251-264. https://doi.org/10.1016/S0738-081X(97)00205-8

Ponka, P., 1997. Tissue-specific regulation of iron metabolism and heme synthesis: distinct control mechanisms in erythroid cells. *Blood,* **89**: 1-25. https://doi.org/10.1182/blood.V89.1.1

Rozen, S. and Skaletsky, H., 2000. Primer3 on the WWW for general users and for biologist programmers. *Methods Mol. Biol.,* **132**: 365-386. https://doi.org/10.1385/1-59259-192-2:365

Šali, A., Potterton, L., Yuan, F., van Vlijmen, H. and Karplus, M., 1995. Evaluation of comparative protein modeling by MODELLER. *Proteins,* **23**: 318-326. https://doi.org/10.1002/prot.340230306

Sarkany, R.P., Ibbotson, S.H., Whatley, S.D., Lawrence, C.M., Gover, P., Mufti, G.J., Murphy, G.M., Masters, G.S., Badminton, M.N. and Elder, G.H., 2011. Erythropoietic uroporphyria associated with myeloid malignancy is likely distinct from autosomal recessive congenital erythropoietic porphyria. *J. Invest. Dermatol.,* **131**: 1172-1175. https://doi.org/10.1038/jid.2011.5

Scarlett, Y.V. and Brenner, D.A., 1998. Porphyrias. *J. Clin. Gastroenterol.,* **27**: 192-198. https://doi.org/10.1097/00004836-199810000-00003

Schneidman-Duhovny, D., Inbar, Y., Nussinov, R. and Wolfson, H.J., 2005. PatchDock and SymmDock: Servers for rigid and symmetric docking. *Nucl. Acids Res.,* **33**: W363-W367. https://doi.org/10.1093/nar/gki481

Schubert, H.L., Phillips, J.D., Heroux, A. and Hill, C.P., 2008. Structure and mechanistic implications of a uroporphyrinogen III synthase product complex. *Biochemistry,* **47**: 8648-8655. https://doi.org/10.1021/bi800635y

Shady, A.A., Colby, B.R., Cunha, L.F., Astrin, K.H., Bishop, D.F. and Desnick, R.J., 2002. Congenital erythropoietic porphyria: Identification and expression of eight novel mutations in the uroporphyrinogen III synthase gene. *Br. J. Haematol.,* **117**: 980-987. https://doi.org/10.1046/j.1365-2141.2002.03558.x

Solis, C., Aizencang, G.I., Astrin, K.H., Bishop, D.F. and Desnick, R.J., 2001. Uroporphyrinogen III synthase erythroid promoter mutations in adjacent GATA1 and CP2 elements cause congenital erythropoietic porphyria. *J. clin. Invest.,* **107**: 753-762. https://doi.org/10.1172/JCI10642

Szlendak, U., Bykowska, K. and Lipniacka, A., 2016. Clinical, biochemical and molecular characteristics of the main types of porphyria. *Adv. clin. exp. Med.,*

25: 361-368. https://doi.org/10.17219/acem/58955

Tanigawa, K., Takamura, N. and Yamashita, S., 1995. Congenital erythropoietic porphyria. *Nihon Rinsho.,* **53**: 1422-1426.

Tezcan, I., Xu, W., Gurgey, A., Tuncer, M., Cetin, M., Öner, C., Yetgin, S., Ersoy, F., Aizencang, G. and Astrin, K., 1998. Congenital erythropoietic porphyria successfully treated by allogeneic bone marrow transplantation. *Blood,* **92**: 4053-4058. https://doi.org/10.1182/blood.V92.11.4053.423k38_4053_4058

Thunell, S., 2000. Porphyrins, porphyrin metabolism and porphyrias. I. Update. *Scand J. clin. Lab. Invest.,* **60**: 509-540. https://doi.org/10.1080/003655100448310

Tsai, S.-F., Bishop, D. and Desnick, R., 1987. Purification and properties of uroporphyrinogen III synthase from human erythrocytes. *J. biol. Chem.,* **262**: 1268-1273.

Urquiza, P., Laín, A., Sanz-Parra, A., Moreno, J., Bernardo-Seisdedos, G., Dubus, P., González, E., Gutiérrez-de-Juan, V., García, S., Eraña, H., 2018. Repurposing ciclopirox as a pharmacological chaperone in a model of congenital erythropoietic porphyria. *Sci. Transl. Med.,* **10**: 7467. https://doi.org/10.1126/scitranslmed.aat7467

Verma, A., Rashidghamat, E., Martinez, A., Fassihi, H. and Sarkany, R., 2014. Congenital erythropoietic porphyria: A case in which symptoms were precipitated by an unrelated anaemia. *Br. J. Dermatol.,* **171**: 422-423. https://doi.org/10.1111/bjd.12945

Warner, C.A., Yoo, H.-W., Roberts, A.G. and Desnick, R.J., 1992. Congenital erythropoietic porphyria: identification and expression of exonic mutations in the uroporphyrinogen III synthase gene. *J. clin. Invest.,* **89**: 693-700. https://doi.org/10.1172/JCI115637

Wiederholt, T., Poblete-Gutierrez, P., Gardlo, K., Goerz, G., Bolsen, K., Merk, H. and Frank, J., 2006. Identification of mutations in the uroporphyrinogen III cosynthase gene in German patients with congenital erythropoietic porphyria. *Physiol. Res.,* **55**: S85-92.

Wood, E.J., 1983. Molecular cloning. A laboratory manual by T Maniatis, E F Fritsch and J Sambrook. pp 545. Cold Spring Harbor Laboratory, New York. 1982. $48 ISBN 0-87969-136-0. *Biochem. Educ.*, **11**: 82-82.

Xu, W., Kozak, C.A. and Desnick, R.J., 1995. Uroporphyrinogen-III synthase: molecular cloning, nucleotide sequence, expression of a mouse full-length cDNA, and its localization on mouse chromosome 7. *Genomics,* **26**: 556-562. https://doi.org/10.1016/0888-7543(95)80175-L

Yisgedu, T.B., Chen, X., Lingam, H.K., Huang, Z., Meyers, E.A., Shore, S.G. and Zhao, J.-C., 2010. Intermolecular dihydrogen-and hydrogen-bonding interactions in diammonium closo-decahydrodecaborate sesquihydrate. *Acta Crystallographr. C.,* **66**: m1-m3. https://doi.org/10.1107/S0108270109040815